NATIONAL ADVISORY COMMITTEE FOR AERONAUTICS

TECHNICAL NOTE 2680

FLAME SPEEDS OF 2,2,4-TRIMETHYLPENTANE-OXYGEN-NITROGEN MIXTURES

By Gordon L. Dugger and Dorothy D. Graab

Lewis Flight Propulsion Laboratory
Cleveland, Ohio

Washington
April 1952

1X

NATIONAL ADVISORY COMMITTEE FOR AERONAUTICS

TECHNICAL NOTE 2680

FLAME SPEEDS OF 2,2,4-TRIMETHYLPENTANE-OXYGEN-NITROGEN MIXTURES

By Gordon L. Dugger and Dorothy D. Graab

2448

SUMMARY

The laminar flame speed of 2,2,4-trimethylpentane with various oxygen-nitrogen mixtures has been determined from schlieren photographs of Bunsen-type flames. Flame-speed data were obtained as a function of equivalence ratio with air at initial temperatures of 311°, 367°, and 422° K and with premixed oxygen-nitrogen mixtures containing 0.250, 0.294, 0.347, and 0.496 mole fraction of oxygen at initial temperatures of 311° and 422° K. Linear relations were found between maximum flame speed U_{max} (cm/sec) and mole fraction of oxygen α for each of the initial temperatures 311° and 422° K. Both lines intercepted the oxygen axis near $\alpha = 0.120$. An empirical equation including both the effect of α and the effect of initial temperature T_0 (°K) was obtained:

$$U_{max} = 0.133\ T_0^{1.40}(\alpha - 0.120)$$

The experimental results for the effect of α were predicted on a relative basis within approximately 20 percent by theories based on either a thermal mechanism, such as that presented by Semenov, or a diffusion mechanism, such as the square-root law presented by Tanford and Pease. This is the same order of agreement as was reported for predictions of the effect of initial temperature on flame speed. Both theories predict curves for the effect of α on U_{max} for which the second derivatives are negative, as compared with linear relations between α and U_{max} observed experimentally. No explanation for the difference in trends between experiment and theory is given. No linear correlations between maximum flame speed and active particle concentrations were found. Such correlations were previously reported in an investigation of the effect of initial temperature on flame speed.

INTRODUCTION

Data for gaseous hydrocarbon fuels have already shown the marked effect of the percentage of oxygen in oxygen-nitrogen mixtures on minimum ignition energy, blow-off and flashback limit, quenching distance, and flame speed (reference 1). Data of this type should give clues as to the importance of reaction kinetics in flame propagation and should yield further information on what the over-all mechanism of flame propagation might be. Furthermore, such data for liquid fuels would be of special interest, because they might assist in the interpretation of the combustion process in aircraft engines; the oxygen-nitrogen ratio is a quantity that can be intentionally varied to produce a considerable effect on combustion properties without greatly affecting such processes as fuel atomization and mixing.

At the NACA Lewis laboratory a program is under way in which some of the combustion properties of 2,2,4-trimethylpentane-oxygen-nitrogen mixtures are being studied. The present report includes data on the laminar flame speeds of homogeneous mixtures of 2,2,4-trimethylpentane with oxygen and nitrogen. Flame speed has been determined as a function of equivalence ratio (fraction of stoichiometric fuel-oxygen ratio) with air at 311°, 367°, and 422° K and with oxygen-nitrogen mixtures containing 0.250, 0.294, 0.347, and 0.496 mole fraction of oxygen at 311° and 422° K. The experimental values of maximum flame speed are compared with the values predicted by theories of flame propagation based on either a thermal or a diffusion mechanism.

SYMBOLS

The following symbols are used in this report:

A	axial cross-sectional area of cone (cm^2)
a_0	number of molecules of combustible per unit volume of initial mixture
B_i	term near unity arising from radical recombination
$C_{v,f}$	molar specific heat at constant volume at flame temperature (cal/(mole)(°K))
$c_{p,f}$	specific heat at flame temperature (cal/(g)(°K))
$\overline{c_p}$	mean specific heat, T_0 to T_f (cal/(g)(°K))
D	diffusion coefficient (cm^2/sec)

D_f	diffusion coefficient at flame temperature (cm^2/sec)
$D_{i,m}$	diffusion coefficient of i^{th} radical at mean combustion zone temperature (cm^2/sec)
$D_{i,r}$	relative diffusion coefficient of i^{th} radical with respect to one of the radicals at initial temperature (dimensionless)
E	activation energy (kcal/g-mole)
exp	base of Napierian logarithmic system raised to power in parenthesis following exp
h	height of cone (cm)
K	collision number from specific rate equation, $k = Ke^{-E/RT}$ ($cm^3/(molecule)(sec)$)
k_i	specific rate constant for reaction between i^{th} radical and combustible material ($cm^3/(molecule)(sec)$)
L_m	total concentration of gas at mean combustion zone temperature ($molecules/cm^3$)
l	slant height or length of generating curve (cm)
M	molecular weight
m	slope of straight line
n_1/n_2	moles of reactants per moles of products from stoichiometric equation
p_H	mole fraction of hydrogen atom in burned gas
p_i	mole fraction of i^{th} radical in unburned gas
p_O	mole fraction of oxygen atom in burned gas
p_{OH}	mole fraction of hydroxyl radical in burned gas
Q	mole fraction of potential combustion product in unburned gas
Q'	mole fraction of combustible in unburned gas
R	gas constant ($kcal/(g\text{-}mole)(^oK)$)

S	lateral surface area (cm^2)
T	absolute temperature (^oK)
T_f	flame temperature (^oK)
T_m	mean combustion zone temperature assumed equal to 0.7 T_f (^oK)
T_0	initial mixture temperature (^oK)
U	flame speed (cm/sec)
U_{max}	maximum flame speed, varying φ at constant α and T_0 (cm/sec)
α	mole fraction of oxygen in oxygen-nitrogen mixture
η	viscosity of mixture (poise)
η_f	viscosity at flame temperature (poise)
θ_m	ratio of mean combustion zone temperature T_m to initial temperature T_0
λ	thermal conductivity ($cal/(cm^2)(sec)(^oK/cm)$)
λ_f	thermal conductivity at flame temperature ($cal/(cm^2)(sec)(^oK/cm)$)
ρ	density of mixture (g/cm^3)
ρ_f	density at flame temperature (g/cm^3)
ρ_0	density of mixture at initial temperature (g/cm^3)
φ	equivalence ratio, fraction of stoichiometric fuel-oxygen ratio

EXPERIMENTAL PROCEDURE

The apparatus is diagrammatically illustrated in figure 1. The experimental procedure may be summarized as follows: The liquid fuel was fed at the desired rate into a heated turbulent stream of oxygen and nitrogen. The resulting gaseous mixture was brought to the desired initial temperature by passage through a coil in an oil jacket, which also heated the burner tube. The mixture was burned as a Bunsen-type flame at atmospheric pressure. Flame speed was determined from schlieren photographs of the flame by a total-area method.

Fuel and oxygen-nitrogen mixtures. - The minimum purity claimed by the supplier of the 2,2,4-trimethylpentane was 99.6 mole percent. Oxygen and nitrogen were obtained premixed, and were analyzed by the supplier to ±0.1 volume percent. For the 21-percent oxygen mixture, laboratory service air containing approximately 0.4 volume percent water was used.

Flow system. - The liquid-fuel feed system was similar to that described in reference 2. Liquid fuel was driven up through a precision-bore tube K (fig. 1) by a mercury column, which in turn was driven by air pressure from the tank O. The air pressure in tank O was increased at a constant rate by metering air through a critical-flow orifice E. The liquid fuel from the tube K was forced into the side arm of a glass capillary tee I. Meanwhile an oxygen-nitrogen mixture was metered, preheated, and passed into the run of the glass capillary tee. The resulting gaseous mixture of fuel, oxygen, and nitrogen passed through a small heated plenum chamber J and into a copper tube, which passed down through the oil jacket of the burner L and connected to the base of the burner tube.

The critical-flow orifices were made by mounting ruby jewel bearings in stainless-steel tubes which were fitted at each end with compression fittings, so that the orifices were easily interchangeable. The orifices were calibrated in place with wet test meters, using service air or oxygen-nitrogen mixture as required.

The fuel feed tube was a 70-centimeter length of precision-bore glass tubing with an inside diameter of 6.414 millimeters. The tube was calibrated with 2,2,4-trimethylpentane by determining the rate of change in the height of the driving mercury column at various gage pressures for a given orifice and known upstream temperature in the pressurizing-air line. For each orifice, a straight-line relation between gage pressure and linear feed rate for a known upstream temperature was determined, from which volumetric feed rate of fuel vapor at initial mixture temperature T_0 and atmospheric pressure could be calculated.

Burner tubes. - The burner tube shown in figure 1 was a 120-centimeter length of brass tubing with an inside diameter of 1.256 centimeters. For the higher oxygen concentrations, it was necessary to use tubes of smaller diameters to avoid flashback. This was accomplished by using a series of smaller insert tubes, each of which had a 3-centimeter-diameter lip at the top, so that it could be soft-soldered to the lip on the 1.256-centimeter tube. These insert tubes were 60-centimeter lengths of brass or stainless-steel tubing having inside diameters of 0.297, 0.617, and 0.838 centimeters. A spacing ring and monel flashback screen were silver-soldered to the upstream end of each insert tube.

Temperature control. - Temperatures were maintained by circulating heated oil throughout the oil-jacketing system. The oil was heated

electrically by 2 three-stage heaters in series. A thermostatic controller was installed in the second heater, which was the smaller of the two. Temperatures were measured by iron-constantan thermocouples installed at the positions shown in figure 1. Temperatures at the burner port were measured periodically by an aspirating thermocouple and were found to be within $1/2^{\circ}$ C of the oil temperature at the inlet to the burner jacket. The oil temperature at the jacket inlet was controlled to $\pm 1^{\circ}$ C.

Optical system. - A two-mirror (Z-type) schlieren system (reference 1, p. 216) with horizontal knife edge was used. A 25-watt concentrated arc lamp served as the light source. The camera lens gave a 1:1 image size. The exposure time was 1/50 second.

Flame-speed measurement. - Flame speeds were determined from the schlieren photographs by the total-area method, wherein the average normal flame speed is equal to the volume rate of flow of the unburned mixture divided by the surface area of the cone formed by the combustion zone. This surface area S was determined by the approximate relation for cone-like surfaces of revolution:

$$S = \pi A l / h \qquad (1)$$

A typical schlieren photograph is shown in figure 2. Measurements were based on the outside of the white edge of the cone. The location of the flame base was defined by the base of the cone image rather than by the burner port. (Note the separation between the cone base and burner tip in fig. 2.) In order to aid in determining the maximum flame speeds, data scatter was diminished by the method described in reference 3 (an averaging method which diminishes errors in measurements for equation (1)); however, essentially the same results would have been obtained without this technique.

EXPERIMENTAL RESULTS

In figure 3(a) flame speed is plotted against equivalence ratio (fraction of stoichiometric fuel-oxygen ratio) for 2,2,4-trimethylpentane-oxygen-nitrogen mixtures for α values $(O_2/(O_2 + N_2))$ of 0.210, 0.250, 0.294, 0.347, and 0.496 at an initial temperature of 311° K and atmospheric pressure (the average atmospheric pressure was 744 mm). Similar data for an initial temperature of 422° K are presented in figure 3(b). Each of the curves in figure 3 exhibits a flame-speed maximum at an equivalence ratio between 1.0 and 1.1. These maximum flame speeds are presented in table I along with values from some additional runs.

In figure 4 maximum flame speed is plotted against α for initial temperatures of 311° and 422° K. It is seen that a linear relation is

obtained for each temperature. The least-squares equations for flame speed U_{max} in centimeters per second as a function of α are as follows:

For 311° K,

$$U_{max} = 409\ \alpha - 51.1 \tag{2}$$

and for 422° K,

$$U_{max} = 601\ \alpha - 69.3 \tag{3}$$

The α-intercepts for zero flame speed indicated are 0.125 for 311° K and 0.115 for 422° K. These values of α are in general agreement with the values indicated by inflammability-limit data for these same mixtures (reference 4). In order to obtain a single empirical equation including the effects of both α and the initial temperature, it was assumed that both lines had α-intercepts of 0.120 and that for each initial temperature

$$U = m(\alpha - 0.120) \tag{4}$$

where the slope m is a function of T_0. For 311° K, $m = 400$ and for 422° K, $m = 613$. At any given α, the slope will be equal to the flame speed divided by a constant. The slope m for equation (4) could be expressed in terms of T_0, if an empirical equation for flame speed as a function of T_0 at some value of α could be obtained. Such an equation was obtained for $\alpha = 0.210$ from the logarithmic plot in figure 5. For this plot the points for 311° and 422° K were obtained using the slopes 400 and 613, respectively, whereas the 367° K point was taken from table I. The three points for $\alpha = 0.210$ fall on a straight line represented by the equation

$$U_{max} = 0.01193\ T_0^{1.40} \tag{5}$$

From which

$$m = \frac{0.01193\ T_0^{1.40}}{0.210 - 0.120} = 0.133\ T_0^{1.40} \tag{6}$$

Substituting equation (6) into equation (4) gives the general equation

$$U_{max} = 0.133\ T_0^{1.40}\ (\alpha - 0.120) \tag{7}$$

which represents the experimental data with a mean deviation of 2.6 percent, as shown by the values in table I. This equation should have engineering usefulness for cases in which initial temperature and oxygen concentrations are in or near the range covered in these experiments.

THEORETICAL PREDICTIONS

It is shown in reference 3 that either the thermal theory equations presented by Semenov (reference 5) or the diffusion theory equation of Tanford and Pease (references 6 and 7) predicted the relative effect of initial mixture temperature on flame speed within approximately 20 percent for the hydrocarbon-air mixtures studies. In the present report, the same equations have been considered for the prediction of the effect of oxygen concentration on flame speed.

Thermal theory. - The thermal theory equation for a bimolecular reaction controlling is (reference 5):

$$U = \sqrt{\frac{2\lambda_f\ K\ a_0\ c_{p,f}^2}{\rho_0\ \overline{c_p}^3} \left(\frac{T_0}{T_f}\right)^2 \left(\frac{\lambda}{c_p\ \rho\ D}\right)_f^2 \left(\frac{n_1}{n_2}\right)^2 \left(\frac{RT_f^2}{E}\right)^3 \frac{\exp(-E/RT_f)}{(T_f - T_0)^3}} \tag{8}$$

By use of this equation, point-by-point calculations were made for predicted maximum flame speeds, relative to the experimental value for $\alpha = 0.210$, at the four higher values of α studied experimentally. The results for initial temperatures of 311° and 422° K are presented in table II and figure 6(a). The values of the physical properties were estimated from data available in the literature, as described in the following paragraphs. In all cases it was assumed that ideal gas mixtures were obtained, for which the physical properties were additive.

Theoretical adiabatic flame temperatures were obtained by the matrix method of reference 8, using heats of formation and heat content functions from references 9 and 10. Viscosity values at flame temperature were obtained by extrapolation of data given in reference 11. Thermal conductivity values at flame temperatures were obtained using this viscosity data and the relation (reference 1, p. 415)

$$\lambda_f = \left(\frac{\eta_f}{M}\right)\left(C_{v,f} + \frac{9}{4}\ R\right)$$

where $C_{v,f}$ data were obtained by interpolation of values from reference 9. Mean specific heat values between T_0 and T_f were calculated from data in reference 9. It was assumed that the diffusion coefficients were proportional to η/ρ.

For an essentially stoichiometric reactant mixture, either the initial fuel concentration or the initial oxygen concentration could be used for a_0 in equation (8) to predict the relative effect of oxygen concentration on flame speed. Both fuel and oxygen are consumed in the same proportions and the relation between reaction-zone concentration and initial concentration should be the same for oxygen as for fuel (reference 5, p. 39).

A value of 40 kilocalories per gram-mole has been arbitrarily chosen for the over-all activation energy. This value has been used in thermal theory calculations for 32 hydrocarbon fuels (reference 12). Adiabatic compression data have been reported from which an apparent activation energy of 32 kilocalories was obtained (reference 1, p. 188). However, this value was determined on the basis of computed temperatures uncorrected for cooling by the walls, so that it is low. In order to show the importance of E in the thermal theory results, curves for both 40 and 32 kilocalories are presented in figure 6(a). The greatest difference appears at the higher values of α (farthest from the datum value); for example, at $\alpha = 0.496$ and $T_0 = 422^\circ$ K, the predicted maximum flame speed is approximately 13 percent low with $E = 40$ and approximately 26 percent low with $E = 32$.

The temperature dependence of the collision number in the reaction rate equation was not considered by Semenov. The effect is small compared to the exponential term since the collision number is proportional to the square root of the reaction temperature (reference 13). Thus for $\alpha = 0.496$ and $T_0 = 422^\circ$ K, the predicted flame speeds would be increased by approximately 5 percent, making the value for $E = 40$ now 8 percent low and for $E = 32$ now 22 percent low.

Diffusion theory. - The equation given by Tanford and Pease (reference 6, p. 863), which they have termed "the square-root law", may be written in the form

$$U = \sqrt{\sum_i k_i p_i D_{i,m} L_m \frac{Q'}{QB_i} \frac{1}{\theta_m^2}} \qquad (9)$$

Since the effect of α on flame temperature is relatively large, the temperature dependence of the specific rate constant k_i should be considered. The activation energies for the reactions between active

particles and fuel molecules are probably of the order of 5 to 15 kilocalories per gram-mole. An approximate value of 10 kilocalories is quoted for the reaction

$$H + C_8H_{18} \rightarrow C_8H_{17} + H_2$$

in reference 14. The activation energies for the reaction of O and OH might be somewhat smaller. Therefore, an average value of 7 kilocalories has been arbitrarily chosen and is assumed to hold for H, O, and OH particles. The temperature dependence of k_i would then be expressed by

$$k_i \propto \exp\ (-E/RT_m)$$

$$\propto \exp\left(\frac{-7}{R(0.7\ T_f)}\right)$$

$$k_i \propto \exp\ (-5000/T_f)$$

As was assumed in the thermal theory discussion,

$$D \propto \frac{\eta}{\rho} \propto T^{1.84}$$

and therefore

$$D_{i,m} \propto D_{i,r}\ \theta_m^{1.84}$$

The molecular concentration factor L_m is inversely proportional to T_m. Approximate calculations were made which indicate that, for the present purpose, the factor Q'/QB_i may be ignored with an error of less than 4 percent. The effect of oxygen concentration on flame speed predicted by equation (9) is therefore given by

$$U \propto \sqrt{\sum_i p_i\ D_{i,r}\ \frac{\exp\ (-5000/T_f)}{T_m\ \theta_m^{0.16}}}$$

from which, at a given initial temperature,

$$U \propto \sqrt{\sum_i p_i D_{i,r} \frac{\exp(-5000/T_f)}{T_f^{1.16}}} \qquad (10)$$

where

$$\sum_i p_i D_{i,r} = 6.5 p_H + p_{OH} + p_O$$

Values computed from equation (10) are presented in table II and figure 6(b). Also plotted in figure 6(b) is the curve which results from neglecting the temperature dependence of k_i (zero activation energy). It should be noted that the temperature dependence of the collision number in k_i is again neglected, as it was in the Semenov equation. The effect of including it would be as discussed previously. It may be seen from figure 6(b) that equation (10) predicts relative flame speed within approximately 20 percent. When the temperature dependence of k_i is neglected, the predictions are within approximately 5 percent of the experimental values.

In reference 3 linear correlations between maximum flame speed and either $(6.5 p_H + p_{OH} + p_O)$ or p_H alone were obtained for gaseous mixtures of constant composition but varying initial temperature. No such correlations were found for the present data with varying oxygen concentrations (see fig. 7). In reference 15 linear relations were observed between flame speed and $\sqrt{6.5 p_H + p_{OH} + p_O}$ when equivalence ratio was varied for a given hydrocarbon-air system at room temperature. For the present data, maximum flame speed (at essentially constant equivalence ratio) varies linearly with $\sqrt{6.5 p_H + p_{OH} + p_O}$ up to $\alpha = 0.347$, but the flame speed at $\alpha = 0.496$ is greater than the value indicated by extrapolation of this linear relation, as shown in figure 7.

Both the thermal theory and the diffusion theory predict curves for the relative effect of α on U_{max} for which the second derivatives are negative. No explanation can be given for the difference between the experimental and the theoretically predicted trends at present.

In conclusion, either the thermal theory as presented by Semenov or the diffusion theory of Tanford and Pease predicts the effect of oxygen concentration on flame speed within approximately 20 percent. Beginning with the assumptions that thermal equilibrium and adiabatic flame temperatures are attained, the relative agreement in either case depends largely on the treatment of the temperature dependence of the rate constant.

SUMMARY OF RESULTS

A study of the laminar flame speeds of homogeneous mixtures of 2,2,4-trimethylpentane with oxygen and nitrogen at 311° and 422° K gave the following results:

1. The maximum flame speed increased linearly with oxygen concentration at a given initial temperature. The following equations for maximum flame speed U_{max} in centimeters per second as a function of mole fraction of oxygen in the oxygen-nitrogen mixture α were obtained:

For 311° K,

$$U_{max} = 409\ \alpha - 51.1$$

And for 422° K,

$$U_{max} = 601\ \alpha - 69.3$$

2. Both flame speed-concentration lines intercepted the α axis at a value near 0.120. For the small temperature range of 311° to 422° K an empirical equation including both the effect of initial temperature and the effect of oxygen concentration expressed as $(\alpha - 0.120)$ on maximum flame speed was obtained:

$$U_{max} = 0.133\ T_0^{1.40}\ (\alpha - 0.120)$$

3. Either the thermal theory as presented by Semenov or the diffusion theory of Tanford and Pease predicted the relative effect of oxygen concentration on maximum flame speed within approximately 20 percent. Theoretical adiabatic flame temperatures and equilibrium radical concentrations were computed by a matrix method; when these values were used, the relative agreement between experimental and theoretically predicted flame speeds depended largely on the treatment of the temperature dependence of the reaction rate constants in either theory. In general, the agreement was of the same order as that previously reported for the effect of initial mixture temperature on flame speed.

4. Both the thermal and the diffusion theory predicted curves for the effect of α on U_{max} for which the second derivatives were negative, as compared with the linear relation between α and U_{max} observed experimentally. This difference in trends between experiment and theory cannot be explained at present.

5. No linear correlations between maximum flame speed and active particle concentrations were obtained. Such correlations were found in the previous initial-temperature investigation.

Lewis Flight Propulsion Laboratory
National Advisory Committee for Aeronautics
Cleveland, Ohio, January 9, 1952

REFERENCES

1. Lewis, Bernard, and von Elbe, Guenther: Combustion, Flames, and Explosions of Gases. Academic Press, Inc. (New York), 1951.

2. Calcote, Hartwell F.: Accurate Control and Vaporizing System for Small Liquid Flows. Anal. Chem., vol. 22, no. 8, Aug. 1950, pp. 1058-1060.

3. Dugger, Gordon L.: Effect of Initial Mixture Temperature on Flame Speed of Methane-Air, Propane-Air, and Ethylene-Air Mixtures. NACA TN 2374, 1951.

4. Spakowski, Adolph E., and Belles, Frank E.: Variation of Pressure Limits of Flame Propagation With Tube Diameters for Various Isooctane-Oxygen-Nitrogen Mixtures. NACA RM E52A08.

5. Semenov, N. N.: Thermal Theory of Combustion and Explosion. III - Theory of Normal Flame Propagation. NACA TM 1026, 1942.

6. Tanford, Charles, and Pease, Robert N.: Theory of Burning Velocity. II. The Square Root Law for Burning Velocity. Jour. Chem. Phys., vol. 15, no. 12, Dec. 1947, pp. 861-865.

7. Tanford, Charles: The Role of Free Atoms and Radicals in Burner Flames. Third Symposium on Combustion and Flame and Explosion Phenomena, The Williams & Wilkins Co. (Baltimore), 1949, pp. 140-146.

8. Huff, Vearl N., and Morrell, Virginia E.: General Method for Computation of Equilibrium Composition and Temperature of Chemical Reactions. NACA TN 2113, 1950.

9. Anon.: Selected Values of Properties of Hydrocarbons. Circular C461. Nat. Bur. Standards, Nov. 1947.

10. Huff, Vearl N., and Gordon, Sanford: Tables of Thermodynamic Functions for Analysis of Aircraft-Propulsion Systems. NACA TN 2161, 1950.

11. Hirschfelder, J. O., Bird, R. B., and Spotz, Ellen L.: Viscosity and Other Physical Properties of Gases and Gas Mixtures. Trans. A.S.M.E., vol. 21, no. 8, Nov. 1949, pp. 921-937.

12. Walker, P. L., Jr., and Wright, C. C.: Hydrocarbon Flame Velocities Predicted by Thermal Versus Diffusional Mechanisms. Paper presented at 120th Meeting Am. Chem. Soc. (New York), Sept. 3-7, 1951. (See Abstracts of Papers 120th Meeting of Am. Chem. Soc., p. 9-I.)

13. Glasstone, Samuel: Text-Book of Physical Chemistry. D. Van Nostrand Co., Inc. (New York), 1940, pp. 1072-1073.

14. Steacie, E. W. R.: Atomic and Free Radical Reactions. Reinhold Pub. Corp., 1946, p. 520.

15. Simon, Dorothy M., and Wong, Edgar L.: Flame Velocities over a Wide Composition Range for Pentane-Air, Ethylene-Air, and Propyne-Air Flames. NACA RM E51H09, 1951.

TABLE I - EXPERIMENTAL, LEAST SQUARES, AND EMPIRICAL EQUATION VALUES OF MAXIMUM FLAME SPEED

$\alpha \left(\frac{O_2}{O_2+N_2}\right)$	Initial mixture temperature T_0 (°K)	Stream-flow Reynolds number	Tube diameter (cm)	Maximum flame speed (cm/sec)		
				Experimental	Least squares line (equations (2) and (3))	Empirical $0.133T_0^{1.40}(\alpha-0.120)$ (equation (7))
0.210	311	1000	1.256	34.6	34.9	36.1
.250	311	1000	.838	52.1	51.2	52.1
.294	311	1600	.838	72.2	69.2	69.7
.294	311	900	.617	67.2	69.2	69.7
.347	311	1200	.617	89.1	90.9	90.9
.496	311	1800	.297	152.2	151.9	150.6
.210	367	1000	1.256	44.8	-----	45.3
.210	422	1000	1.256	56.1	56.8	55.2
.210	422	1000	1.256	59.0	56.8	55.2
.210	422	700	.838	57.4	56.8	55.2
.250	422	1400	.838	83.1	80.8	79.8
.294	422	900	.617	108.0	107.2	106.7
.294	422	900	.617	102.1	107.2	106.7
.347	422	1400	.617	138.0	139.1	139.3
.496	422	1800	.297	229.9	228.5	230.7

TABLE II - THEORETICALLY-PREDICTED VALUES OF MAXIMUM FLAME SPEED RELATIVE TO EXPERIMENTAL VALUE FOR MOLE FRACTION OF OXYGEN $\alpha = 0.210$

$\alpha \left(\frac{O_2}{O_2+N_2}\right)$	Initial mixture temperature T_0 (°K)	Flame temperature T_f (°K)	Equivalence ratio φ	Equilibrium radical concentrations (mole fraction)			Maximum flame speed (cm/sec)		
				p_H	p_{OH}	p_O	Thermal theory E=40 kcal	Square-root law E=7 kcal	Experimental least squares
0.210	311	2285	1.05	0.000643	0.00241	0.000257	34.9[a]	34.9[a]	34.9
.250	311	2447	1.05	.00179	.00586	.00105	52.0	59.4	51.2
.294	311	2562	1.02	.00336	.01081	.00275	67.5	83.6	69.2
.347	311	2670	1.02	.00626	.01711	.00543	88.2	113.5	90.9
.496	311	2850	1.00	.01599	.03538	.01577	134.7	181.7	151.9
.210	422	2337	1.05	.000887	.00319	.000415	56.8[a]	56.8[a]	56.8
.250	422	2487	1.05	.00226	.00696	.00141	82.1	91.6	80.8
.294	422	2595	1.02	.00401	.01209	.00334	105.4	125.1	107.2
.347	422	2697	1.02	.00717	.01856	.00627	132.8	166.4	139.1
.496	422	2870	1.00	.01737	.03694	.01713	199.6	259.5	228.5

[a]Experimental values.

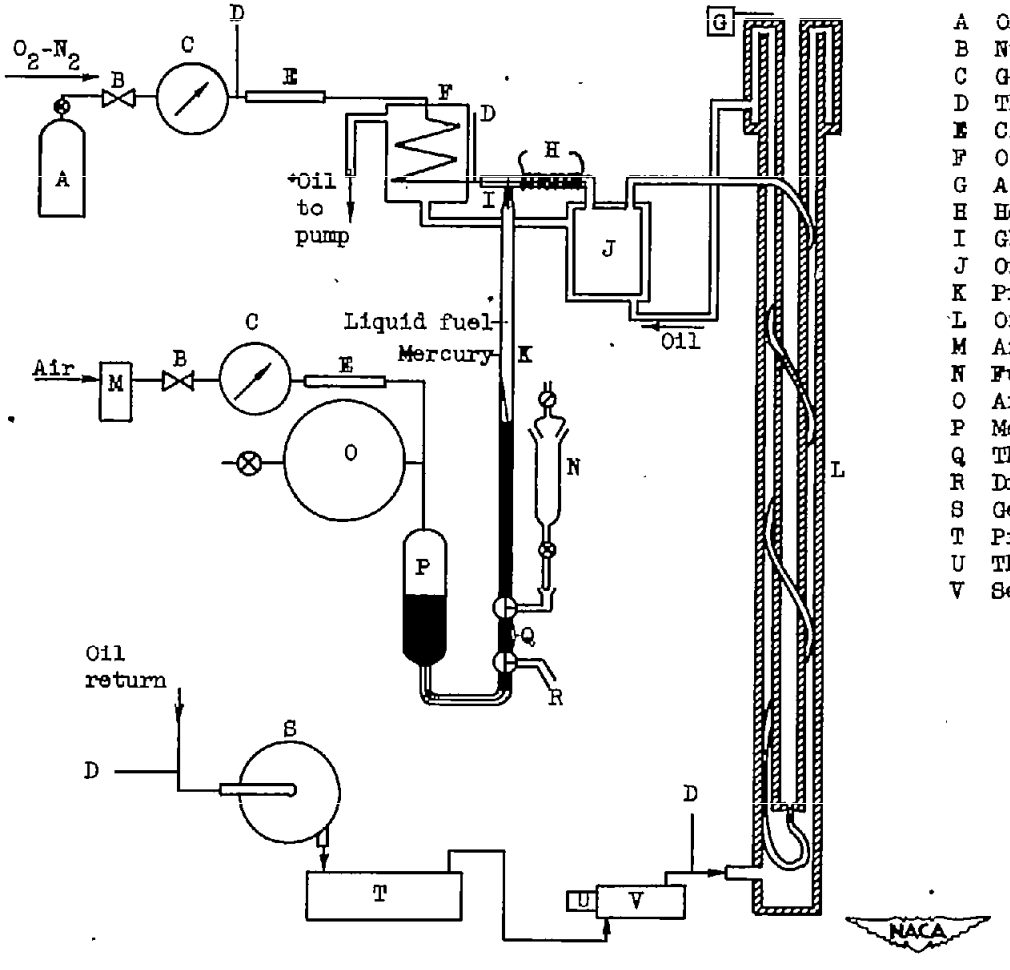

A Oxygen-nitrogen mixture cylinder
B Nullmatic pressure regulator
C Gauge, 0-100 lb/sq in.
D Thermocouple
E Critical flow orifice
F Oil bath for oxidant
G Aspirating thermocouple for port
H Heating coil
I Glass capillary tee
J Oil-jacketed plenum chamber
K Precision-bore tube
L Oil-jacketed burner tube
M Air filter
N Fuel-storage tube
O Air chamber
P Mercury reservoir
Q Three-way stopcock
R Drain
S Gear pump
T Primary oil heater
U Thermostatic controller
V Secondary oil heater

Figure 1. - Diagrammatic sketch of experimental apparatus.

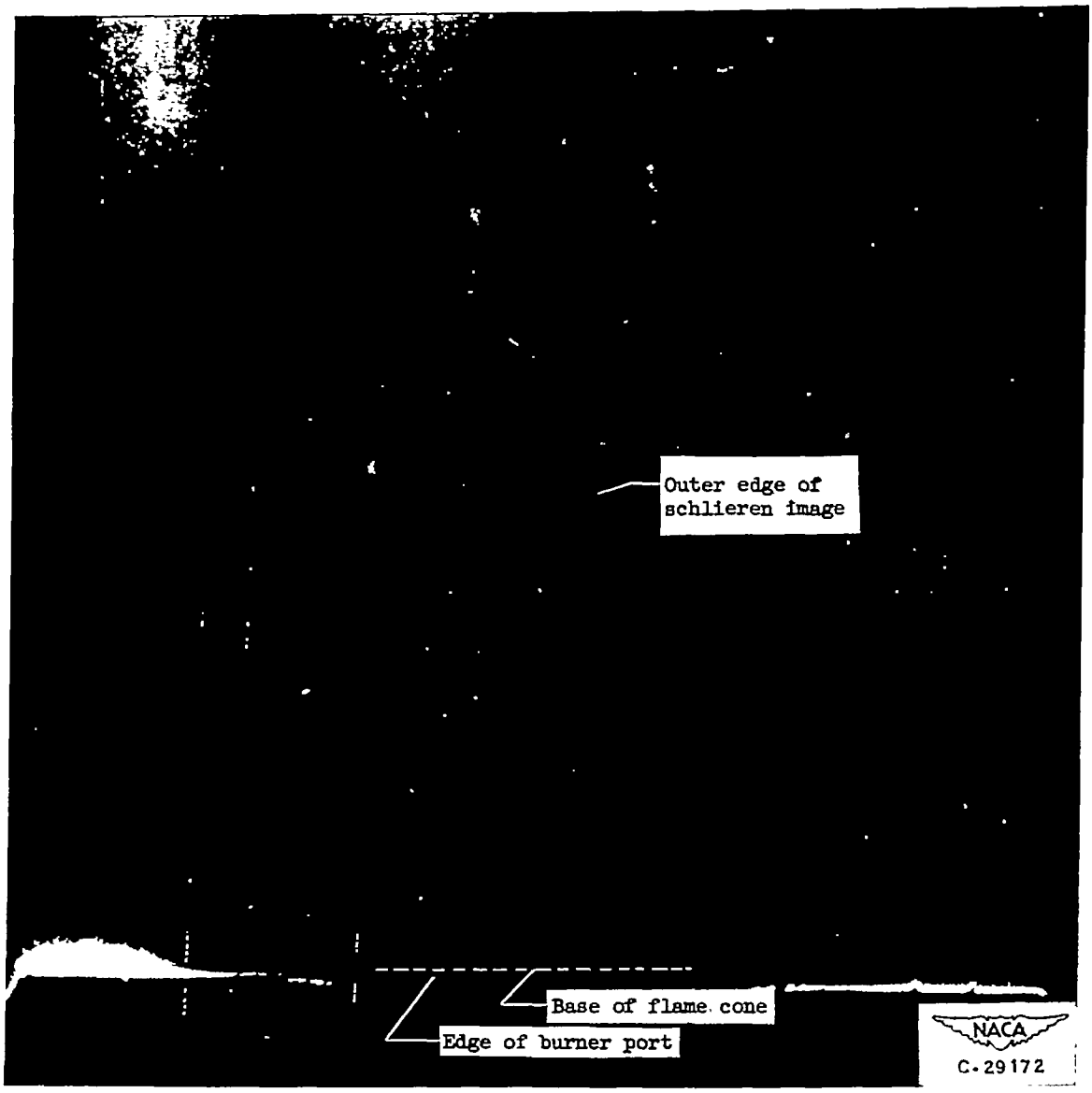

Figure 2. - Typical schlieren photograph showing outer edge and base of flame cone image.

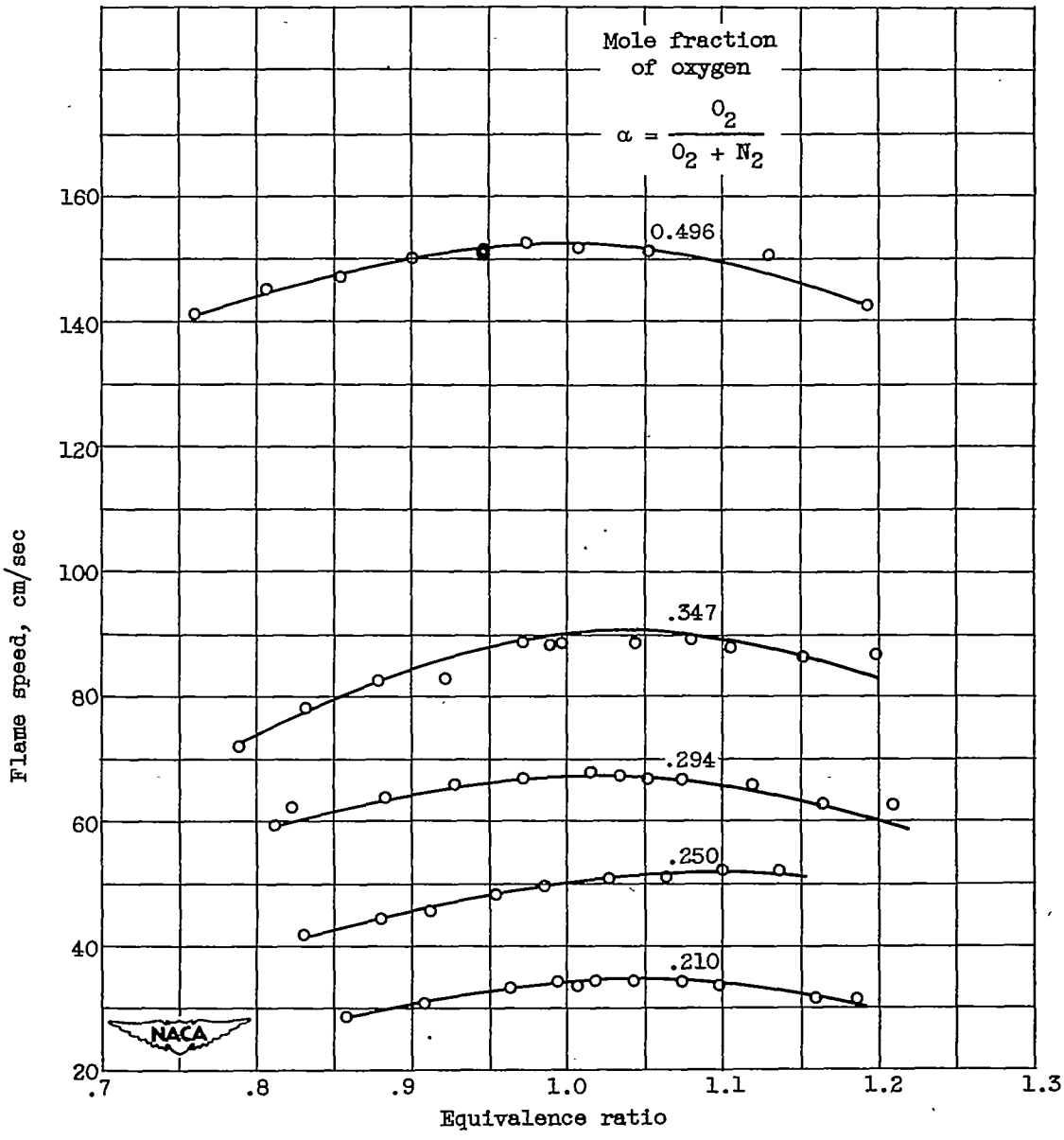

(a) Initial temperature, 311° K.

Figure 3. - Flame speeds of 2,2,4-trimethylpentane-oxygen-nitrogen mixtures.

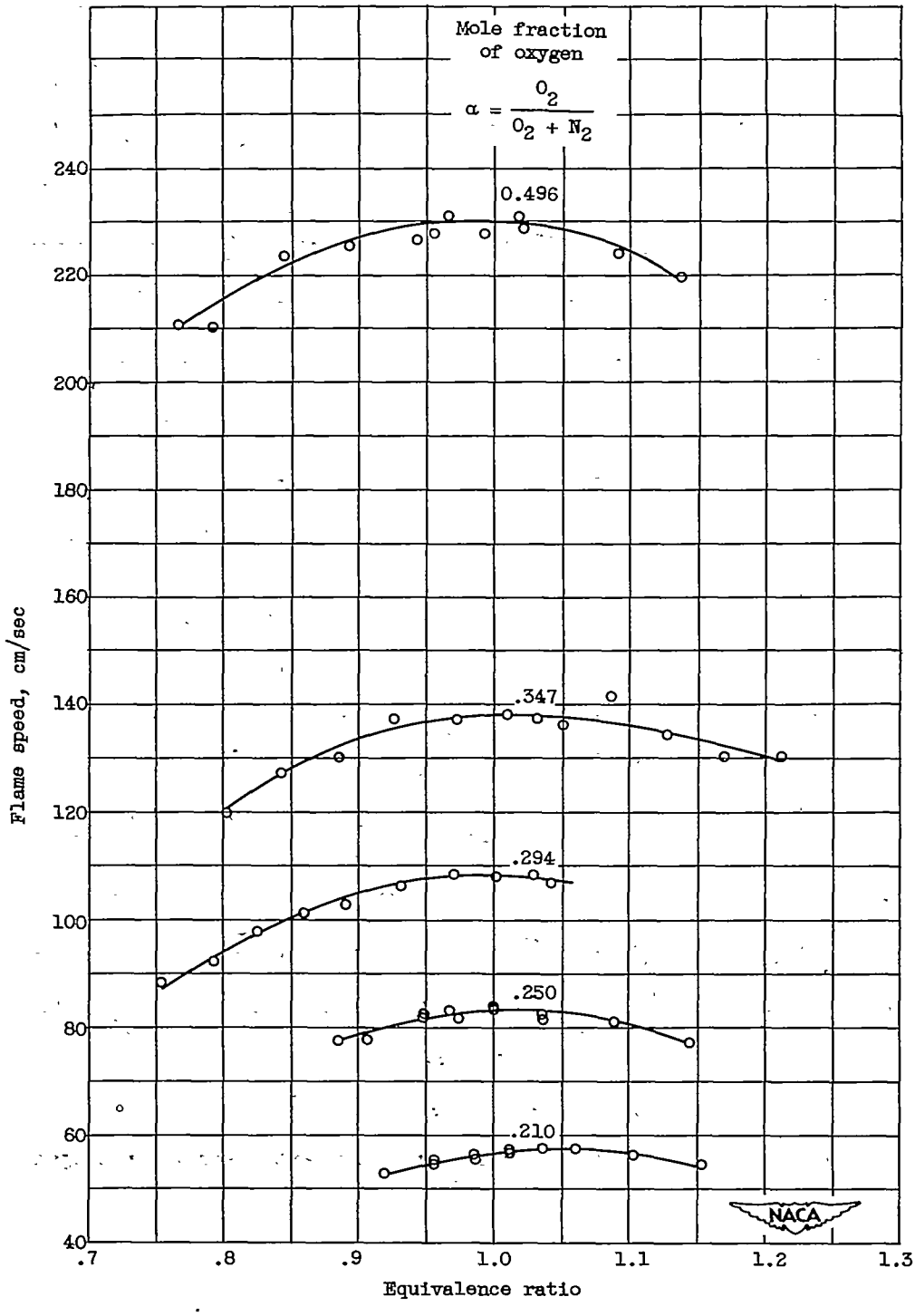

(b) Initial temperature, 422° K.

Figure 3. - Concluded. Flame speeds of 2,2,4-trimethylpentane-oxygen-nitrogen mixtures.

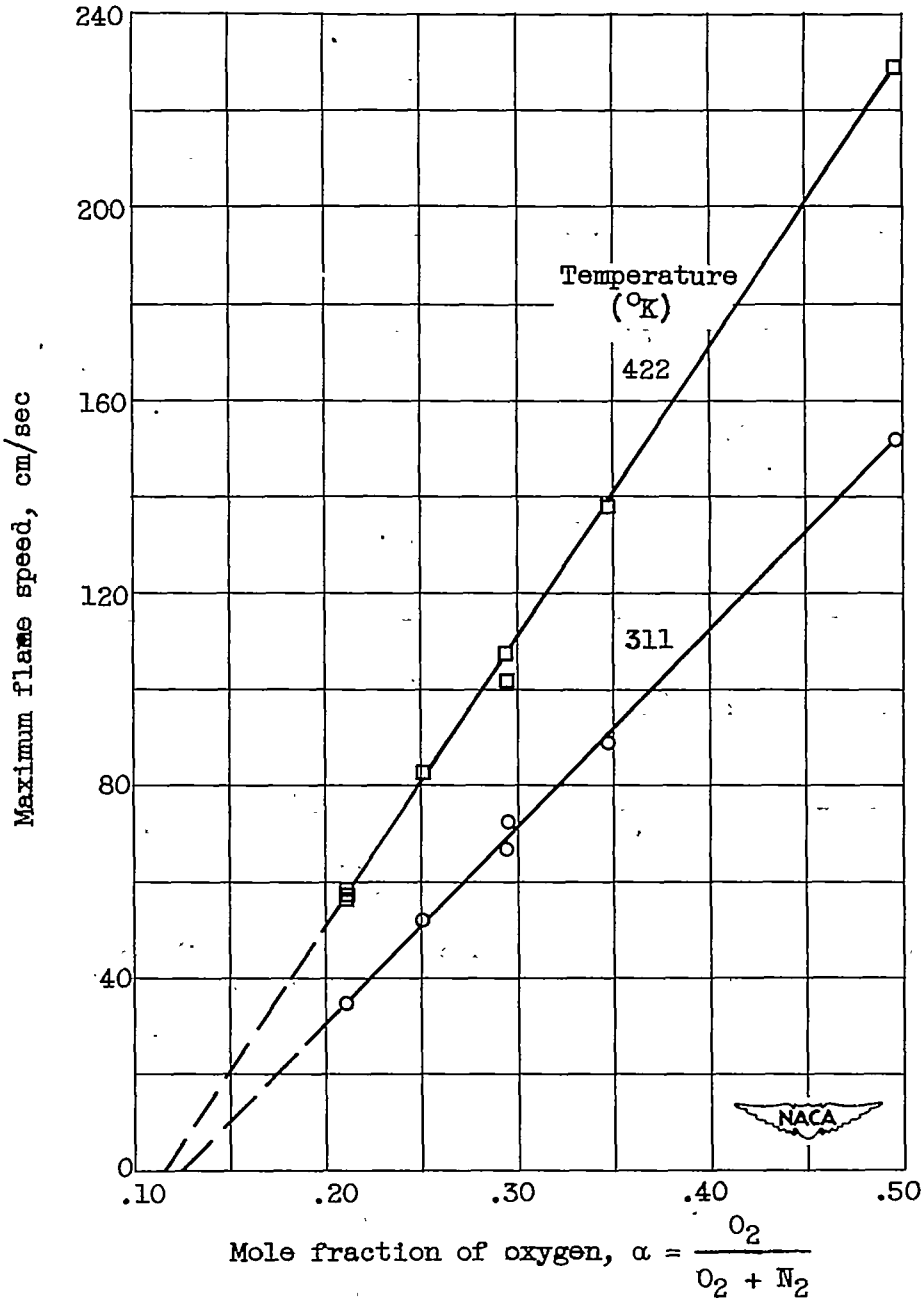

Figure 4. - Effect of oxygen concentration on maximum flame speeds of 2,2,4-trimethylpentane-oxygen-nitrogen mixtures at 311° and 422° K.

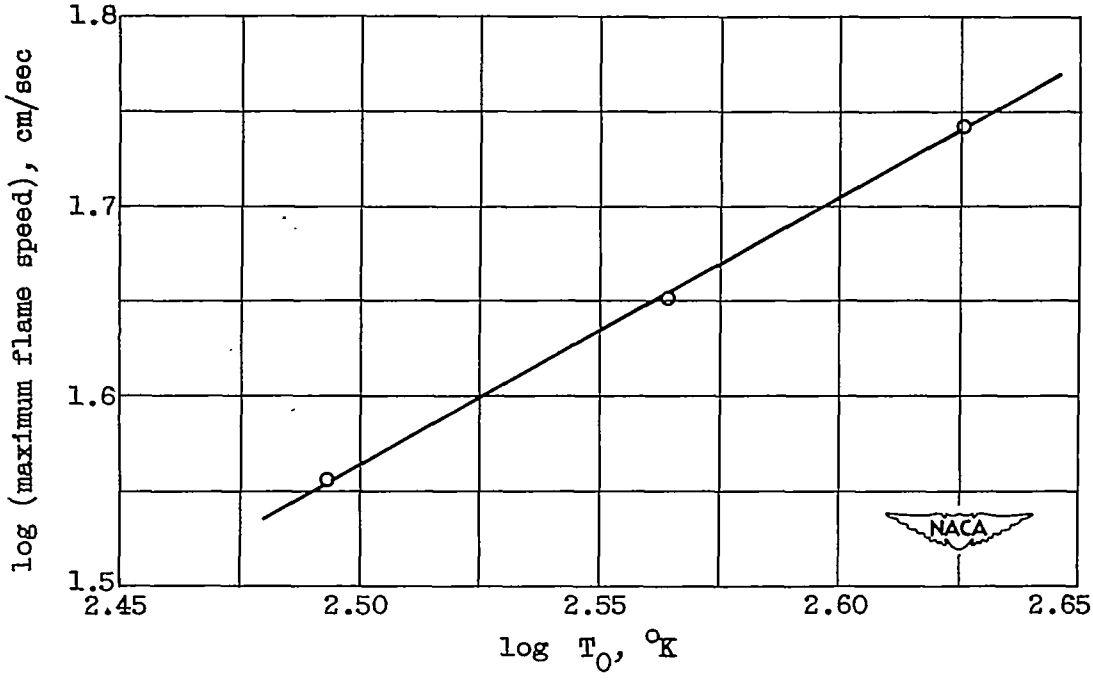

Figure 5. - Effect of temperature on maximum flame speed for 2,2,4-trimethylpentane-air mixtures. $\alpha = 0.210$.

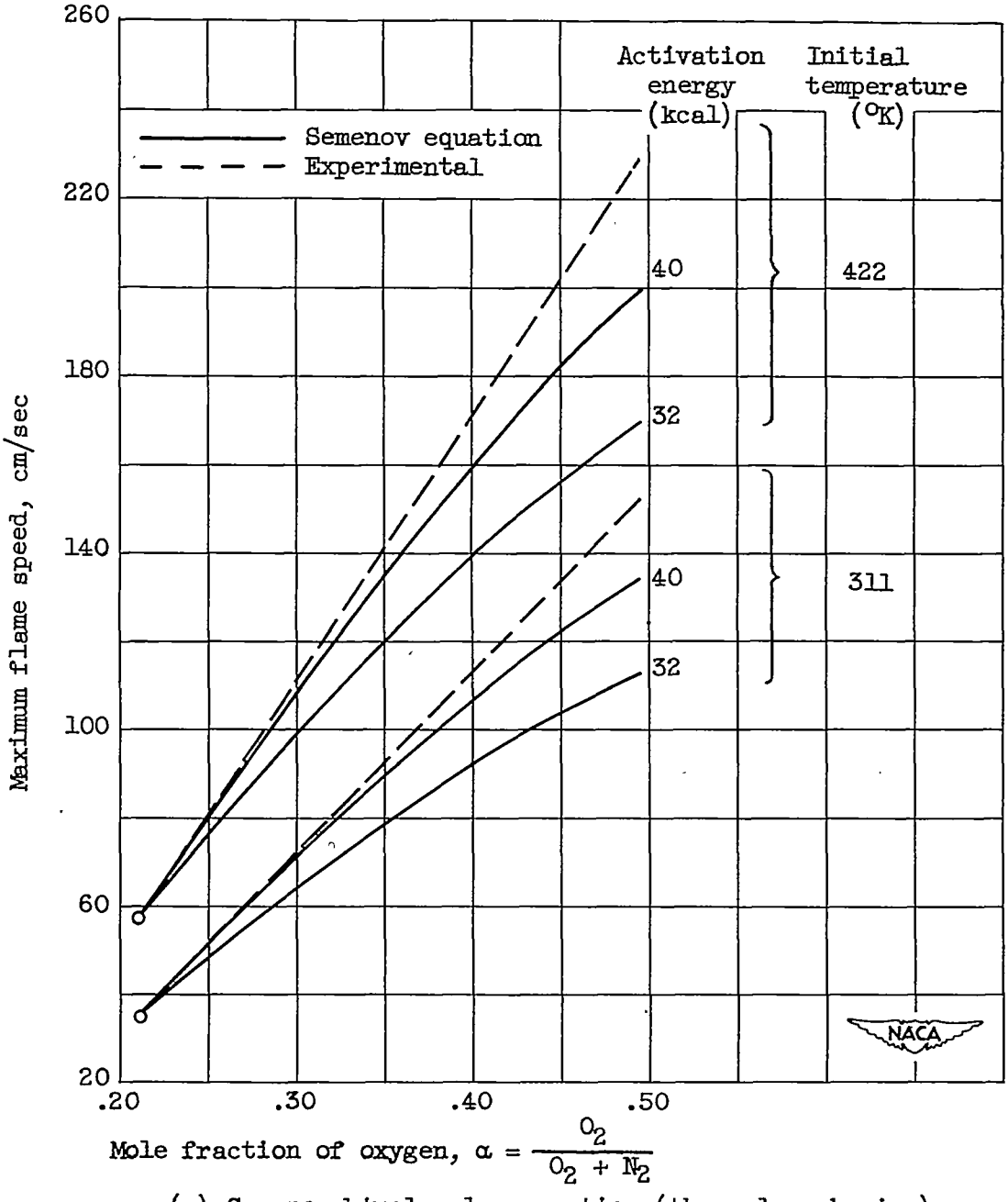

(a) Semenov bimolecular equation (thermal mechanism).

Figure 6. - Effect of oxygen concentration on maximum flame speeds of 2,2,4-trimethylpentane-oxygen-nitrogen flames. Comparison of theoretically predicted curves (relative basis) with experimental results.

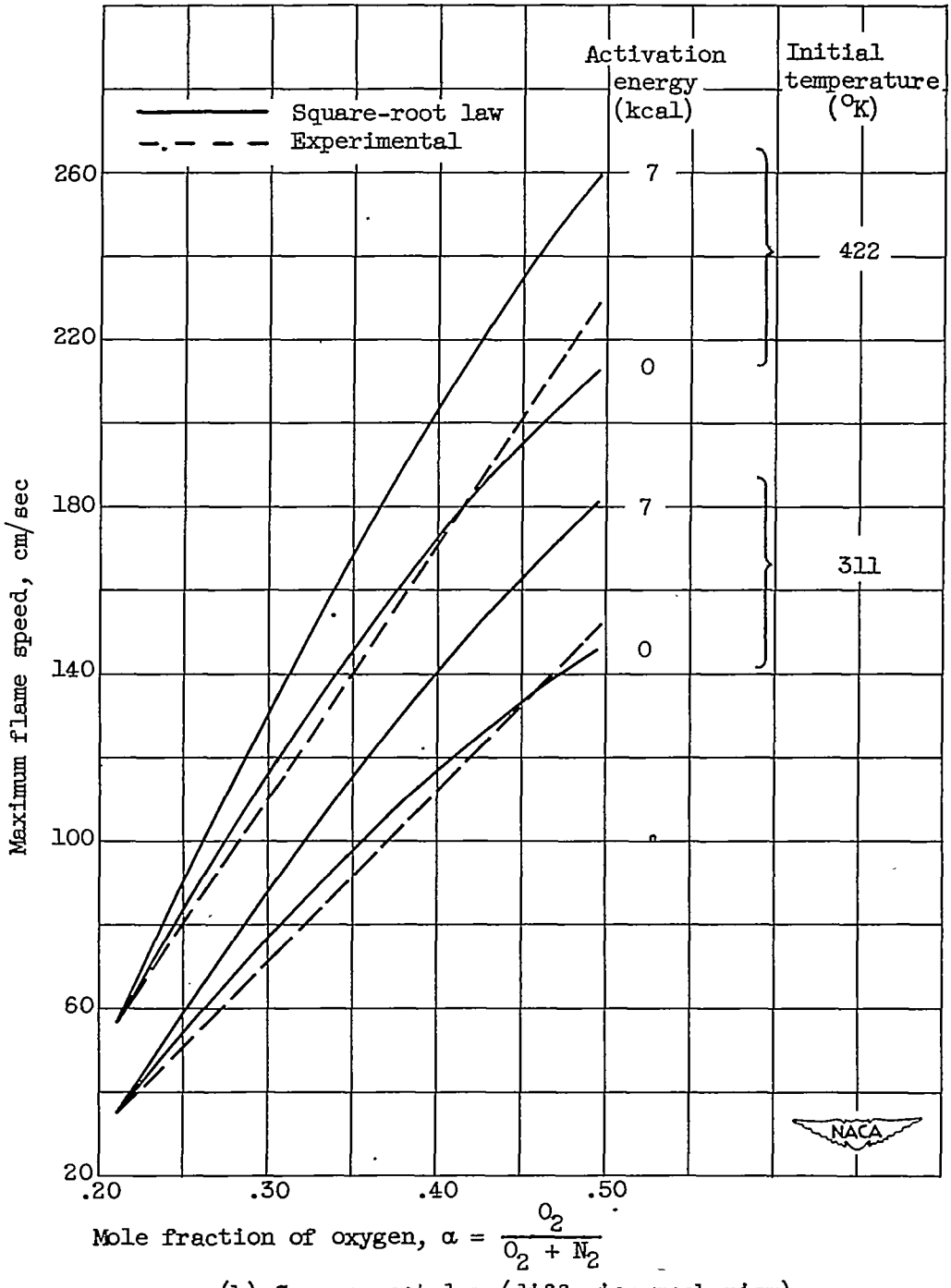

(b) Square-root law (diffusion mechanism).

Figure 6. - Concluded. Effect of oxygen concentration on maximum flame speeds of 2,2,4-trimethylpentane-oxygen-nitrogen flames. Comparison of theoretically predicted curves (relative basis) with experimental results.

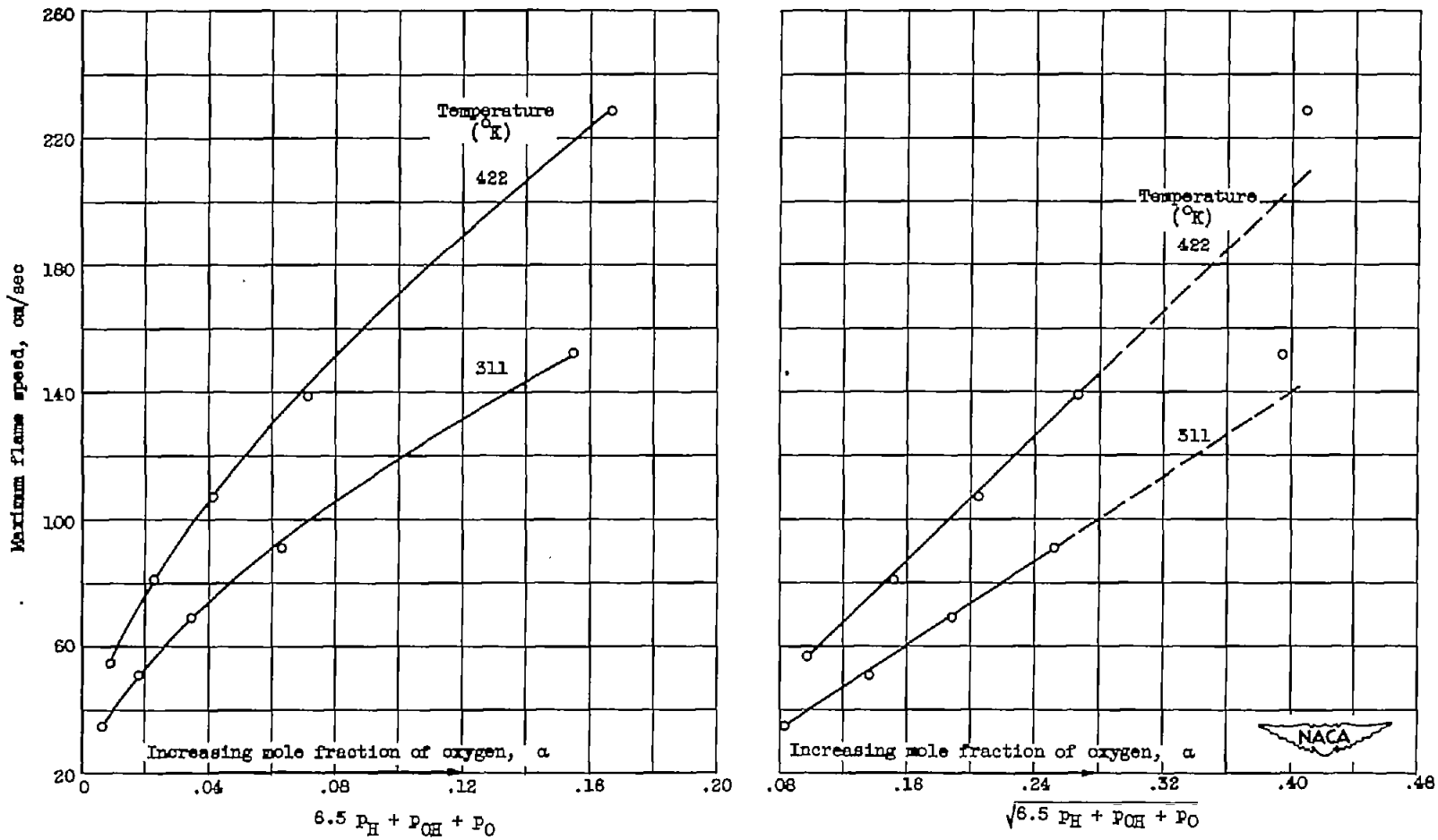

Figure 7. - Relation between maximum flame speeds and effective active particle concentrations where mole fraction of oxygen $\alpha = \frac{O_2}{O_2 + N_2}$ is 0.210, 0.250, 0.294, 0.347, and 0.498.